ELSEVIER

Materials Science and Engineering A237 (1997) 216–223

MATERIALS SCIENCE & ENGINEERING A

Ferrite formation in Fe–C alloys during austenite decomposition under non-equilibrium interface conditions

Gerben P. Krielaart, Jilt Sietsma *, Sybrand van der Zwaag

Laboratory of Materials Science, Delft University of Technology, Rotterdamseweg 137, 2628 AL Delft, The Netherlands

Received 28 November 1996; received in revised form 14 April 1997

Abstract

The growth of ferrite during the decomposition of supersaturated austenite in binary Fe–C alloys is studied using a numerical model that allows non-equilibrium conditions at the moving α–γ-interface. A numerical method is presented to account for non-equilibrium interface conditions during diffusional growth. In this model, the driving force for interface migration is given by the difference of the chemical potentials of the austenitic and the ferritic Fe-lattice at the interface. Carbon rearrangement, resulting from the movement of the interface, affects the driving force for interface migration during the transformation, thus establishing a mixed mode of growth control. The mode of control is predicted to vary from essentially a diffusion controlled mode at very low undercooling towards essentially an interface controlled mode at deep undercoolings. The results from this model are in good agreement with several sets of experimental growth rates and the carbon concentration profiles of partially transformed Fe–C alloys. © 1997 Elsevier Science S.A.

Keywords: Phase-transformation kinetics; Interface mobility; Mixed-mode growth control; Fe–C alloys

1. Introduction

The transformation $\gamma \rightarrow \alpha$ in Fe–C alloys and carbon steels involves a change of the Fe lattice from an f.c.c. symmetry (austenite, γ) into a b.c.c. symmetry (ferrite, α). This phase transformation is a heterogeneous process, starting mainly at austenite grain boundaries, and results in a clearly distinguishable α–γ-phase interface during the transformation. If the carbon content of the alloy exceeds the maximum solubility of carbon in ferrite, the transformation involves a rearrangement of carbon through carbon diffusion. In the literature, the growth kinetics of pro-eutectoid ferrite formation in Fe–C alloys and carbon steels is often modelled assuming thermodynamic equilibrium conditions at the α–γ-interface, the so-called local-equilibrium assumption (e.g. Refs. [1–6]). In this case, the volume diffusion velocity of carbon is rate limiting for the growth kinetics. The interfacial reaction, which transforms the f.c.c. lattice into the b.c.c. lattice, is assumed to occur at such a rate that this process can be considered of no importance for the growth kinetics of the transformation. The growth kinetics is then said to be diffusion controlled.

The other extreme in modelling the $\gamma \rightarrow \alpha$-phase transformation is to assume an infinitely fast diffusion of carbon in austenite. In other words, no carbon concentration gradients occur in the γ-phase. The growth is governed by the rate at which f.c.c. iron transforms into bcc iron, which is reflected in the intrinsic mobility of the interface. The growth kinetics is then said to be interface controlled.

In this work a mixed-mode model is proposed for Fe–C steels, taking quantitatively into account both the carbon diffusion and the interface mobility. Experimental evidence exists, for instance recent in situ Transmission Electron Microscopy observations [7], that the ferrite growth rate involves various and continuously changing displacement modes of the interface. The interface clearly does not behave as the transparent, highly flexible barrier the local equilibrium models assume it to be. Such evidence indicates that a finite interface mobility does play a role in the growth kinetics. The mixed-mode model follows, in a one-dimensional model system, the progress of the phase transformation as a function of time, during which the carbon concentration profile is evaluated continuously.

* Corresponding author.

PII S0921-5093(97)00365-1

The carbon concentration profile is determined by the diffusion rate on the one hand, and the interface velocity on the other. The interface velocity in its turn depends on the carbon concentrations on both sides of the interface, since in the model it is assumed that the interface velocity is a combined result of the intrinsic interface mobility and the net driving force for the transformation at the interface. In general, the present approach leads to non-equilibrium conditions at the interface. In the extreme cases of an infinitely large interface mobility or an infinitely large carbon diffusivity, the mixed-mode model approaches the diffusion-controlled or the interface-controlled model, respectively. The accompanying carbon concentrations are characterised by local equilibrium at the interface, and the absence of carbon gradients in the austenite, respectively.

In the paper, the results of model calculations are compared with different types of experimental data on the $\gamma \rightarrow \alpha$-phase transformation. The overall agreement is satisfactory, and is in the Discussion shown to be significantly better than modelling under local-equilibrium conditions would result in.

2. The mixed-mode model

2.1. Theoretical background

Ferrite exhibits a much lower carbon solubility than austenite. If the alloy carbon content is larger than the maximum carbon solubility of ferrite, the movement of the α–γ-interface during the formation of ferrite from austenite involves the transfer of carbon atoms from ferrite to austenite. The carbon rejected by the ferrite and transferred into the austenite causes a carbon mass flux $J_{\alpha\rightarrow\gamma}$ across the interface, given by

$$J_{\alpha\rightarrow\gamma} = (c^{\gamma}(x_{\mathrm{int}}) - c^{\alpha}(x_{\mathrm{int}}))\cdot v, \tag{1}$$

where $c^{\gamma}(x)$ and $c^{\alpha}(x)$ are the carbon concentrations of austenite and ferrite as a function of the position x, respectively. x_{int} represents the position of the interface. The interface velocity is given by v. Carbon diffusion in the ferrite is assumed to take place at such a rate that the carbon is homogeneously distributed. This assumption is justified by the diffusion coefficient of carbon in ferrite [8] being larger than that in austenite [9]. In the austenite a diffusive carbon flux J_{D} occurs, described by Fick's first law:

$$J_{\mathrm{D}} = -D\cdot\left(\frac{\mathrm{d}c^{\gamma}}{\mathrm{d}x}\right), \tag{2}$$

where D is the diffusion coefficient of carbon in austenite. The net carbon flux ΔJ at the interface is given by the difference of the two fluxes:

$$\Delta J = (c^{\gamma}(x_{\mathrm{int}}) - c^{\alpha})\cdot v + D\cdot\left(\frac{\mathrm{d}c^{\gamma}}{\mathrm{d}x}\right)_{x=x_{\mathrm{int}}}. \tag{3}$$

This equation reflects the interaction between carbon diffusion and interface mobility that is taken into account in the mixed-mode model of the ferrite growth. Note that the net carbon flux ΔJ is not necessarily zero at all stages of the transformation. A non-zero value for ΔJ results in a change in the carbon concentration at the interface. The development of the carbon concentration at the interface during the growth is thus determined by both the interface velocity and the diffusive flux. In turn, both these quantities depend on the carbon concentration at the interface. Eq. (3) therefore gives the essentials of the present mixed-mode approach.

In Fig. 1 a schematic representation is given of the carbon concentration profile during the transformation, and of the manner in which it is influenced by the interface velocity and the diffusivity. The dashed line gives the concentration profile for infinitely fast carbon diffusion in austenite. The carbon that is transferred from ferrite to austenite due to the progress of the interface, is redistributed instantaneously over the austenite. Due to the finite dimensions of the austenite grain, an overall increase of the carbon concentration takes place. This increase causes a gradual decrease of the growth velocity. The other extreme, the carbon concentration profile in case of an infinitely large interface mobility, is given by the dotted line in Fig. 1. At

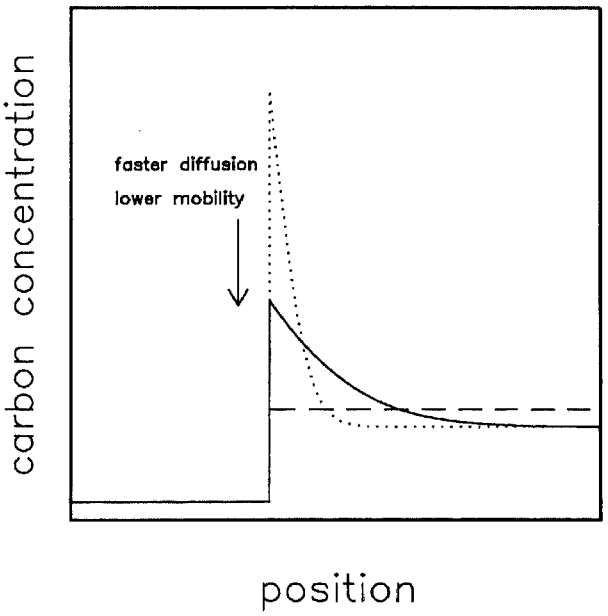

Fig. 1. Schematic carbon concentration profiles at the α–γ-interface for a finite austenite grain. The dotted line gives the profile for local-equilibrium conditions (slow diffusion, high interface mobility), the dashed line for interface-controlled transformation (fast diffusion, low interface mobility), the solid line for the intermediate conditions that the mixed-mode model takes into account.

the interface the carbon concentration in the austenite reaches its equilibrium value, and local-equilibrium conditions are attained at the interface. The solid line in Fig. 1 gives the more general case of mixed-mode growth, as discussed in this paper. The carbon concentration profile, including the carbon concentration at the interface, is determined by both D and v. As is indicated in the figure, the carbon concentration at the interface decreases with increasing D and with decreasing interface mobility. When the carbon concentration gradient extends over the entire grain, the finite grain size has a significant effect on the conditions at the interface, thus influencing the growth kinetics. These so-called soft-impingement effects are also adequately taken into account in the model treated in this paper.

In the evaluation of the mixed-mode concept, information on the diffusivity is readily available [9], but the interface velocity v poses a potential problem. According to the theory of thermally activated growth [10], the interface velocity is determined by the free energy gain of the system. However, since the transfer of the interstitial carbon from the forming ferrite to the austenite is expected to be much faster than the lattice change of the iron, we assume that the chemical potential difference between the Fe-lattice in the ferritic and in the austenitic state constitutes the free energy gain that determines the interface velocity. The interface velocity is given by [11]

$$v = M\Delta\mu_{Fe}, \tag{4}$$

where M is the interface mobility and $\Delta\mu_{Fe}$ the chemical potential difference of iron, which is given by

$$\Delta\mu_{Fe} = \mu^{\gamma}_{Fe}(c^{\gamma}) - \mu^{\alpha}_{Fe}(c^{\alpha}). \tag{5}$$

The chemical potentials μ^{γ}_{Fe} and μ^{α}_{Fe} at the interface depend on the local carbon concentrations in austenite and ferrite, respectively. Both c^{γ} and c^{α} are to be evaluated at the α–γ-interface. The simplicity of Eq. (4) implies that a multitude of structural aspects that influence the mobility, like the degree of coherency of the interface, pinning effects, build-up of stresses, or solute drag, are united in a single mobility parameter M, which is therefore to be interpreted as an effective interface mobility. In this work, the chemical potentials are described using the regular solution sublattice model, originally due to Hillert and Staffansson [12], using the parameters as determined by Gustafson [13]. The mobility of a disordered α–γ-interface has recently been estimated from an analysis of the heat effects accompanying the $\gamma \rightarrow \alpha$ transformation in low-Mn Fe–Mn alloys [11]. For low-alloy compositions, it was found to be essentially independent of the alloy composition. The intrinsic interface mobility M is described by an Arrhenius-type temperature dependence:

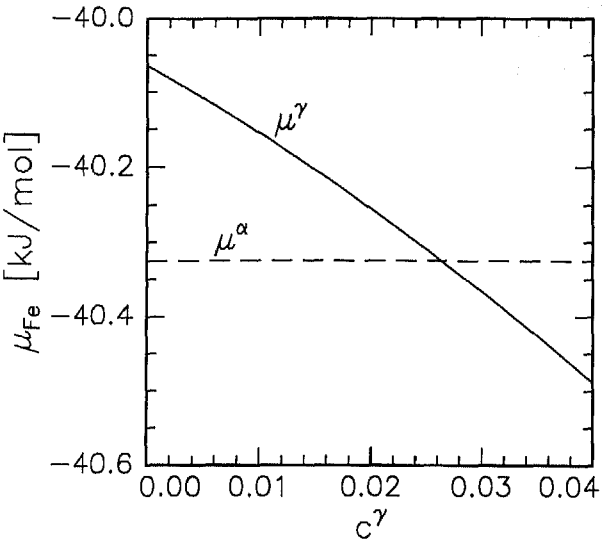

Fig. 2. The chemical potential for Fe in γ-Fe at $T = 1025$ K as a function of the carbon concentration in the austenite. The iron chemical potential for α-Fe at the equilibrium carbon content is also given.

$$M = M_0 \exp\left(-\frac{E}{RT}\right). \tag{6}$$

From the work in Ref. [11], for the activation energy E the value 140 kJ mol^{-1} is used, and the pre-exponential factor M_0 is taken as 58 mm mol (J s)$^{-1}$. RT has its usual meaning. The value for the activation energy is in agreement with experimental observations in pure iron [14]. The value of the pre-exponential factor M_0 is very much lower than the value of 5000 m mol (J s)$^{-1}$ obtained by Hillert [14]. The reasons for this apparent discrepancy are twofold: (1) the observations by Hillert mainly concerned grain growth or recrystallisation in a single phase, and therefore transitions that do not involve volume changes; (2) the influence of manganese, which is known to have a strongly retarding effect on the transformation.

Fig. 2 gives an example, at $T = 1025$ K, of the dependence of μ^{γ}_{Fe} on c^{γ}. The α-line gives the chemical potential for α-Fe containing the equilibrium amount of carbon at this temperature ($c^{\alpha} = 0.0009 = 0.2$ mass% C). The austenite phase is in equilibrium with this ferrite for $c^{\gamma} = 0.0264$ ($= 0.569$ mass% C). If the austenite concentration at the interface is lower than the equilibrium value, a positive $\Delta\mu_{Fe}$ results, and the ferrite grows. The interface velocity v is evaluated by means of the Eqs. (4)–(6). Fig. 2 shows the two competitive processes in the transformation: diffusion of carbon from the interface to the bulk of the austenite tends to reduce c^{γ} at the interface, but this increases the interface velocity, and hence the supply rate of carbon from the ferrite to the austenite at the interface.

As will be shown in the Discussion of this paper, the dependence of both the interface velocity and the diffu-

sive flow on the carbon concentration profile causes a gradual formation of the profile during the growth process, contrary to local-equilibrium models. This effect has a significant influence on the growth kinetics as a function of the degree of transformation.

2.2. Numerical implementation

The model presented in the previous section is applied to the growth kinetics of pro-eutectoid ferrite in supersaturated austenite. The ferrite is assumed to grow by a flat α–γ-interface. The former austenite grain boundary is assumed to be entirely occupied with ferrite nuclei, as is the customary assumption for simple austenite geometry models [3].

The numerical model is one-dimensional, with the x-direction ($0 < x < 1/2d$, with d the austenite grain size) divided into N segments of width Δx. The choice of the austenite grain size d and the number of segments N fixes the segment width Δx ($N = 500$ in the calculations with $d = 50$ μm, and $N = 2000$ with $d = 250$ μm). As stated before, the carbon concentration in the ferrite is assumed to be independent of x, and equal to the equilibrium concentration at the temperature considered. The diffusion coefficient of carbon in austenite is taken from Ref. [9], and increases with increasing carbon concentration. In order to account for the finite austenite grain size, a mirror image is applied for $1/2d < x < d$, which is implemented by the boundary condition $(\partial c^{\gamma}/\partial x)_{x=d/2} = 0$.

The procedure to calculate the migration of the α–γ-interface during the transformation starts with the carbon homogeneously distributed throughout the austenite grain. At $t = 0$ the first segment is transformed into ferrite, during which the surplus amount of carbon is moved into the second segment. The interface velocity is computed according to the Eqs. (4)–(6), where c^{α} is taken either according to the $\alpha/(\alpha+\gamma)$ phase boundary (above the A_1-temperature) or the $\alpha/(\alpha+\theta)$ phase boundary of the Fe–C diagram (below the A_1-temperature). The choice of c^{α} has a minor effect on $\Delta\mu_{Fe}$ [15]. The resulting velocity v determines the time step through $\Delta t = \Delta x/v$. Therefore, in the calculations Δx is constant, and Δt varies according to the momentary interface velocity. Using Eq. (3) for the interface and Eq. (2) for the interior of the remaining austenite, the carbon flux in the austenite is calculated, which results in the carbon concentration profile after the time step Δt. Then, the ferrite phase advances a step Δx, and the calculation loop is repeated. This iterative process is continued until either the austenite grain is completely transformed into ferrite, or the interface velocity has reduced to zero. In that case, as can be understood from Fig. 2, equilibrium has been attained.

3. Experimental validation

3.1. Optical microscopy

Specimens of a high-purity Fe–C alloy with a nominal carbon content of 0.20 ± 0.03 mass% C were partially transformed at an isothermal transformation temperature of 973 K after austenitising for 10 min at 1273 K. To ensure a well-defined thermal cycle, the transformation experiments were carried out using a Bähr dilatometer (type 805A, with a quenching equipment) with S-type thermocouples spot-welded on the surface of the samples. The samples were tubular shaped with a length of 10 mm and a wall thickness of approximately 0.25 mm. Transformation times of 3, 5 and 12 s were used, followed by a quench to room temperature using He-gas. Typical cooling rates during quenching were 200 K s^{-1}.

The thickness of the allotriomorphic ferrite layer in the partially transformed specimens was determined by means of a light-microscopical analysis of the microstructure. This analysis was carried out using a Leitz CBA 8000 quantitative image analysis system connected to a Zeiss Jenavert microscope (equipped with 20 × 0.40 and 50 × 0.80 planachromatic objectives) through a colour CCD camera (500 × 582 pixels). The samples were ground and polished with 1 μm diamond paste and subsequently chemically etched with 1% Nital etchant for a time of 10 s. Sample preparation was completed by the deposition of a layer of ZnTe for use with monochromatic light (wavelength 550 nm). This treatment yielded an enhanced optical contrast between the various constituents of the microstructure. In Fig. 3 the average thickness of the ferrite layers as a function of time, as determined from the microstructure, are compared with the interface positions as computed numerically for a Fe–0.20 mass% C alloy, with $d = 50$ μm, and an isothermal transformation temperature of 973 K.

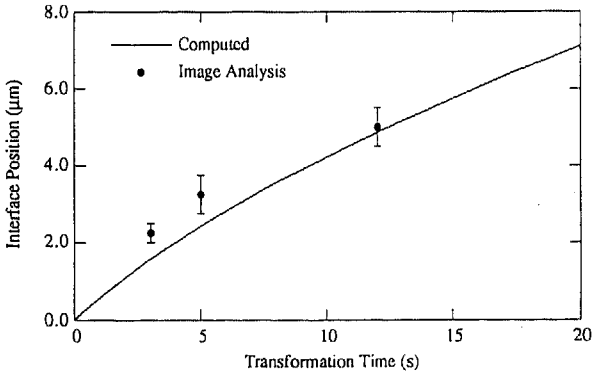

Fig. 3. The average thickness of the ferrite layer as a function of time during isothermal transformation at $T = 973$ K of Fe–0.20mass%C, determined by means of quantitative image analysis. The solid line gives the result of the model calculations.

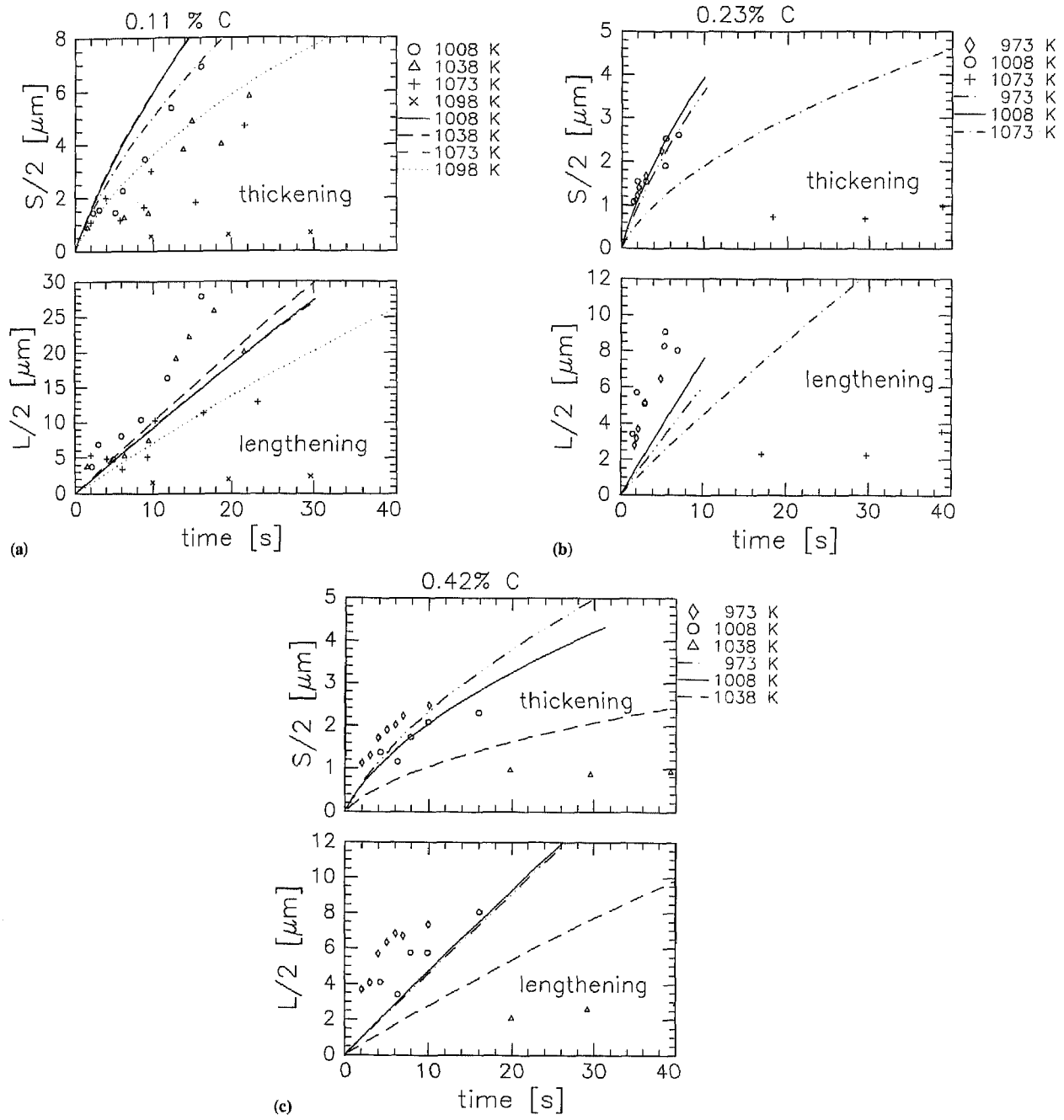

Fig. 4. Thickening and lengthening of ferrite particles in Fe–0.11mass%C (a), Fe–0.23mass%C (b), Fe–0.42mass%C (c). The symbols give the experimental data, taken from Bradley et al. [16], the lines represent the model calculations.

3.2. Ferrite growth perpendicular to and along austenite grain boundaries

An extensive set of experimental growth data has been reported by Bradley et al. [16] for the ferrite growth kinetics in Fe alloys containing 0.11 mass%, 0.23 mass%, 0.42 mass% C, in the temperature range 973–1113 K. All samples had been austenitised at 1573 for 30 min, which resulted in a grain size of approximately 250 μm. Bradley et al. distinguished the growth kinetics perpendicular to the austenite grain boundary ('thickening') and along the austenite grain boundary ('lengthening'). The evolution of the thickness S and of the length L of a typical ferrite grain determined experimentally as a function of time at different temperatures [16] is given in Fig. 4. In order to enable a direct comparison with the modelling of an advancing interface, the data are given as $S/2$ and $L/2$, respectively.

The experimental data of Fig. 4 are compared with the advancement of the α–γ-interface calculated with

the mixed-mode model. For the modelling of the thickening data, the volume diffusion coefficient for carbon in austenite [9] was used; for the modelling of the lengthening data, grain-boundary diffusion of carbon was assumed to be the dominant diffusion mechanism. Since no experimental data for grain-boundary diffusion of carbon in austenite are available in the literature, the diffusion coefficients are calculated using the customary principle that the activation energy for grain-boundary diffusion in metallic systems is half the activation energy for volume diffusion. Lacking information on the pre-exponential factor for grain-boundary diffusion, we took it equal to the pre-exponential factor for volume diffusion. The influence of these choices is limited, since at these high diffusion rates it is the interface mobility that determines the growth rate. In agreement with the actual grain size, in the modelling the grain size is set to 250 μm.

The curves in Fig. 4 give the results of the model calculations. At all but the highest transformation temperatures a reasonable agreement with the experimental data is found for the thickening data. For most temperatures, the calculations slightly underestimate the growth rate for the 0.42 mass% C alloy, and lead to an overestimation of the growth rate for the 0.11 mass% C alloy. The growth rate at the highest transformation temperatures is strongly overestimated by the model. The very strong reduction of the experimental growth rate with increasing temperature seems to indicate that the experimental temperatures are closer to the actual A_3-temperature than theoretically calculated. The problem concerning the highest transformation temperatures is also found in the lengthening data. In this case, for the other temperatures the growth rate for the 0.11 mass% C alloy is best reproduced by the model, whereas for the higher carbon contents a slight underestimation is found.

In conclusion, the mixed-mode growth model gives a reasonable description of the experimental growth data for iron with different carbon contents. The differences between model and experiment are quantitative rather than qualitative.

4. Discussion

4.1. Growth kinetics according to the mixed-mode model

The development of the carbon concentration profile during the transformation of a Fe–0.20mass%C alloy at 1025 K is shown in Fig. 5. The carbon concentration profile builds up during a considerable period of time. The slowly increasing c^γ at the interface causes the interface velocity to decrease continuously during a

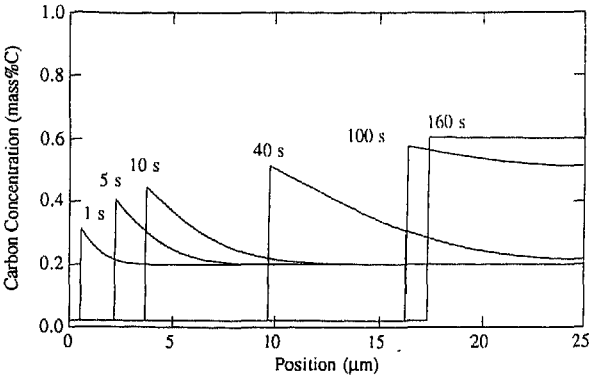

Fig. 5. Carbon concentration profiles computed at various transformation times for an Fe–0.20mass%C alloy transforming at $T = 1025$ K. After 160 s equilibrium has been reached. The austenite grain size in the calculations is 50 μm.

substantial part of the transformation (Fig. 6). Due to this build-up of the carbon concentration profile, the austenite grain size explicitly plays a role in the growth kinetics as modelled by the mixed-mode model. When the interface approaches the middle of the austenite grain, the increased carbon concentration due to the rejection of carbon by the growing ferrite stretches out over the entire remaining austenite, as is beginning to be visible in Fig. 5 at $t = 40$ s. This soft impingement affects the carbon concentration profile, and thereby the growth kinetics. Upon further growth of the ferrite, the carbon concentration at the interface approaches the equilibrium concentration, and the interface velocity drops to zero (Fig. 6). Eventually, the transformation comes to a complete stop when a profile like the '160 s' curve in Fig. 6 has developed. Note that the mass balance for carbon in this situation is mathematically identical to the lever rule for a binary alloy, and

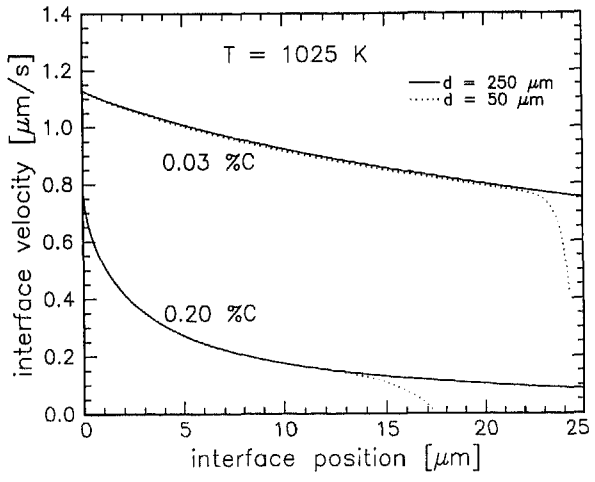

Fig. 6. The calculated interface velocity for two Fe–C alloys at $T = 1025$ K. The figure shows the change in velocity in the course of the transformation, and the influence of the austenite grain size d.

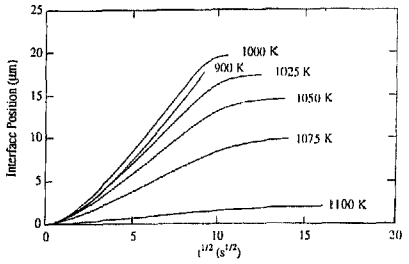

Fig. 7. The calculated interface positions for an Fe–0.20mass%C alloy as a function of the square root of the transformation time at various temperatures ($d = 50$ μm).

the system has therefore reached the equilibrium configuration when it stops.

The temperature dependence of the growth kinetics is rather complex. First, the driving force for interface migration, $\Delta\mu_{Fe}$, depends strongly on the temperature, as well as on the carbon concentration at the interface. In general, this aspect causes the growth rate to increase upon decreasing temperature, i.e. upon larger undercooling. Secondly, the interface mobility itself decreases with decreasing temperature according to Eq. (6), and, thirdly, the carbon diffusivity in austenite also decreases upon decreasing temperature. An additional temperature-dependent factor is the temperature dependence of the equilibrium fractions of austenite and ferrite. Therefore, the temperature dependence of the growth kinetics cannot be summarised in a single relation. For the case of a Fe–0.20mass%C system, the interface position at different temperatures is given in Fig. 7. For the austenite grain size $d = 50$ μm is used, and the final positions of the interface reflect the equilibrium state. In Fig. 7 the interface position as a function of $\sqrt{t}$ shows a distinct linear part, especially in the curves at low undercoolings. At large undercoolings this range of parabolic growth is less pronounced. This is due to the increasingly long initial phase of sub-parabolic growth, during which the carbon pile-up at the interface takes place. The deviation from parabolic growth in the final stage of the curves is due to soft impingement effects.

Finally, the overall carbon content of the material has a significant effect on the transformation kinetics. The composition dependence of the interface velocity at $T = 1025$ K is exemplified in Fig. 6, which, besides the velocity curves for Fe–0.20%C that were treated before, the velocity curves for Fe–0.03%C for $d = 50$ μm and for $d = 250$ μm are given. Clearly, the lower carbon concentration at the interface causes a larger interface velocity (Fig. 2) in the low-carbon alloy. Also, the effect of soft impingement manifests itself at a later stage in low-carbon alloys.

4.2. Mixed-mode model versus local-equilibrium model

Probably the most frequently applied models for transformation kinetics are the models based on the assumption of local equilibrium at the interface. The classical example is Zener's paper of 1949 [1]. The local-equilibrium assumption implies a diffusion-controlled transformation, and the interface position x_{int} as a function of time is given by

$$x_{int} = \alpha\sqrt{Dt}, \tag{7}$$

where α is a dimensionless factor that depends on the equilibrium carbon concentrations, on the overall carbon content, and on the geometry assumed. The carbon diffusivity in ferrite is assumed to be infinitely fast. Eq. (7) is the reason to plot the interface position as a function of $\sqrt{t}$, as we already did in Fig. 7. The local-equilibrium model yields straight lines in such plots (parabolic growth), whereas (see Fig. 7) the mixed-mode model displays a time-dependent slope, although during a substantial part of the transformation parabolic growth does occur.

It is particularly interesting to compare the adequacy of both models with respect to the experimental growth data from Bradley et al. [16] that were given in Fig. 4. Fig. 8 shows both the thickening and the lengthening data for Fe–0.23mass%C as a function of $\sqrt{t}$. The data for the highest temperature have been left out. It is clear that the local-equilibrium model strongly overestimates the growth rate. Whereas in the thickening data

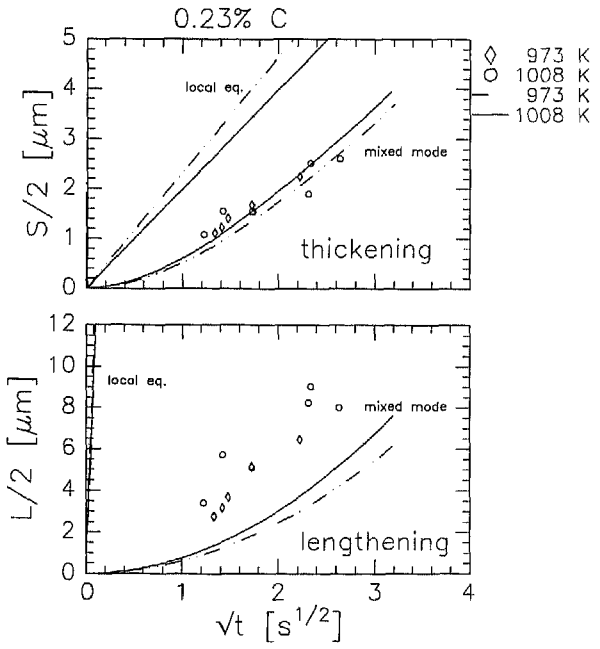

Fig. 8. Comparison of the mixed-mode model and the local-equilibrium model [1] using the data of Fig. 4b. The straight lines apply to the local-equilibrium model, the curved lines to the mixed-mode model.

the difference is moderate, the lengthening data show a marked difference. In fact, the grain-boundary diffusion that plays a role in the lengthening is so fast that a flat carbon concentration profile exists in the austenite throughout the transformation. This means that the growth kinetics for lengthening is essentially interface-controlled, and the composition at the interface is far from the local-equilibrium value. In the kinetics of the thickening, the difference is less pronounced, since the slower diffusion reduces the effect of the limited interface velocity. Nevertheless, a significant discrepancy does exist between the experimental data and the lines for the local-equilibrium model. Fig. 8 shows that the presently used mobility parameters, which were previously obtained for Fe–Mn alloys [11], give a more reasonable account for the effect of the interface mobility for Fe–C alloys than the values for pure iron [14] would. The mobility in pure iron, as reported in Ref. [14], is so high that local equilibrium would be maintained throughout the transformation.

The effect of nucleation on the transformation kinetics has not been taken into account in the present calculations. The agreement between the experimental data and the local-equilibrium model can be improved by allowing an incubation time for nucleation $t_0 \approx 1$ s, and replacing t in Eq. (7) by $(t - t_0)$. The results of the mixed-mode model indicate that the apparent 'slow start' on a $\sqrt{t}$-scale of the transformation that is experimentally observed is not necessarily caused by nucleation processes; it may very well be due to the development of the concentration profiles early in the transformation, as is shown in Fig. 8. Neglecting nucleation in the mixed-mode model calculations has the consequence that the mobility involved is a lowest estimate of the actual mobility.

In conclusion, with the mixed-mode model both thickening and lengthening data are reproduced without adapting the values of the parameters that were previously obtained. The model gives a reasonable reproduction of the growth kinetics in the entire range from diffusion-controlled to interface-controlled transformations. Research that will lead to a further quantification of the interface mobility M (composition dependence, temperature dependence) is currently in progress.

5. Conclusions

The kinetics of diffusional growth of pro-eutectoid ferrite during the decomposition of supersaturated austenite in Fe–C alloys can be satisfactory described using a mixed-mode interface migration model. In this model, the migration of the α–γ-interface is driven by the difference of the chemical potential of the austenitic and the ferritic Fe-lattice at the interface. The austenite carbon concentration at the interface varies with time. This is due to the interaction between the intrinsic α–γ-interface mobility and the carbon volume diffusion in the remaining austenite. This interaction results in an apparent parabolic growth during more advanced stages of transformation. For the interface mobility parameters used (pre-exponential factor $M_0 = 58$ mm mol (J s)$^{-1}$ and activation energy $E = 140$ kJ mol^{-1}), good quantitative agreement between predictions and experimental data for the ferrite growth rate and the carbon concentrations at the interface is obtained, both under conditions where diffusion control prevails and under conditions where interface control prevails.

Acknowledgements

The authors are grateful for financial support from the Innovative Development Project for Metals of the Dutch Ministry of Economic Affairs (IOP-Metalen) and for the financial and experimental support by Hoogovens Corporate Research, IJmuiden, The Netherlands. The contributions of Dr M. Onink, concerning the isothermal transformation experiments and their analysis, as well as the very valuable discussions on the model presented in this paper, and of Ir V.M.M. Silalahi, Mr P.F. Colijn, Dr Ir W.G. Sloof, Ir F. Vermolen and Dr H.K.D.H. Bhadeshia are gratefully acknowledged. The experimental data for Fig. 4 were kindly provided by Professor Aaronson.

References

[1] C. Zener, J. Appl. Phys. 20 (1949) 950.
[2] H.K.D.H. Bhadeshia, L.-E. Svensson, B. Gretoft, Acta Metall. 33 (1985) 1271.
[3] R.A. Vandermeer, Acta Metall. Mater. 38 (1990) 2461.
[4] M. Enomoto, ISIJ Int. 32 (1992) 297.
[5] R.C. Reed, H.K.D.H. Bhadeshia, Mater. Sci. Technol. 8 (1992) 421.
[6] S. Crusius, L. Höglund, U. Knoop, G. Inden, J. Ågren, Z. Metallkde. 83 (1992) 729.
[7] M. Onink, F.D. Tichelaar, C.M. Brakman, E.J. Mittemeijer, S. van der Zwaag, J. Mater. Sci. 30 (1995) 6223.
[8] J. Ågren, Acta Metall. 30 (1982) 841.
[9] J. Ågren, Scr. Met. 20 (1986) 1507.
[10] J.W. Christian, The Theory of Transformations in Metals and Alloys, 2nd ed., Part 1, Pergamon Press, Oxford, 1981, p. 476.
[11] G.P. Krielaart, Ph.D. Thesis, Delft University of Technology, 1995.
[12] M. Hillert, L.-I. Staffansson, Acta Chem. Scand. 24 (1970) 3618.
[13] P. Gustafson, Scand. J. Met. 14 (1985) 259.
[14] M. Hillert, Met. Trans. 6A (1975) 5.
[15] G.P. Krielaart, M. Onink, C.M. Brakman, F.D. Tichelaar, E.J. Mittemeijer, S. van der Zwaag, Z. Metallkde. 85 (1994) 756.
[16] J.R. Bradley, J.M. Rigsbee, H.I. Aaronson, Met. Trans. 8A (1977) 323.